

Redshift dependence of FRB host dispersion measures across cosmic epochs

Sandeep Kumar Acharya,^{a,1} Paz Beniamini^{a,b,c}

^a*Astrophysics Research Center of the Open University, The Open University of Israel, Ra'anana, Israel*

^b*Department of Natural Sciences, The Open University of Israel, P.O Box 808, Ra'anana 4353701, Israel*

^c*Department of Physics, The George Washington University, 725 21st Street NW, Washington, DC 20052, USA*

E-mail: sandeepa@openu.ac.il

ABSTRACT: We constrain the redshift dependence of (rest frame) host galaxy dispersion measures of localized FRBs by assuming it to vary as a simple power law ($\propto (1+z)^\alpha$). We simultaneously fit α as well as the host dispersion measure to the data of FRBs with known redshifts. We find that $\alpha \approx 0$ is preferred over higher values of α with either a positive or negative sign. Such constraints have implications for our understanding of galaxy formation and can be used to inform galaxy and large scale simulations.

¹Corresponding author.

1 Introduction

FRBs (Fast Radio Bursts) are transients with order millisecond durations and typically observed at frequencies in the range of 100 MHz-8 GHz. The first FRB was discovered by [1]. Thousands of FRBs have been discovered to date [2–6] while a few dozens have been identified to a host galaxy and hence have an identified redshift [7, 8]. Additionally, several tens of FRBs have been shown to be repeating in nature [9]. Even with this progress, we still have only a limited understanding of the origin of FRBs. For a review on FRBs, their properties, implications and possible explanations, the readers are referred to the following reviews [8, 10].

The radio pulses from FRBs get dispersed as they travel through ionized medium along the line of sight. The time of arrival of the radio waves is proportional to $DM \cdot \nu^{-2}$ where DM is the dispersion measure which is locally given by $\int n_e dl$, where n_e is the electron density and dl is a line element along the line of sight, which are measured in the rest frame of the medium. The DM measured by the observer is Lorentz transformed from the local source frame by recalling that the DM transforms as the frequency. The observed DM far exceeds the Galactic contribution measured from pulsars. This means that a large fraction of the DM is contributed by propagation of the FRB signals before entering our Galaxy and makes FRBs useful probes for cosmological applications. Also, DM is straightforward to measure and is available with high accuracy for each detected FRB. Several cosmological applications such as determining the baryon contents in the Universe, measuring the Hubble constant and probing the era of reionization have been discussed in the literature [8, 11–17].

The contribution to the observed DM is a combination of DM from the host galaxy, intergalactic medium (IGM), our own Galaxy and the surrounding halo. The IGM term captures the expansion and the baryon content of the Universe. Therefore, it is of primary interest for cosmological applications. However, generally, we do not know the individual components of the total observed DM. Therefore, one needs to have an understanding of the other components in order to extract the maximum cosmological information from given data. Among all the components, the host galaxy is, probably, the most important and complex to understand. It depends upon star formation inside the galaxy as well as baryonic feedback processes. Previous works have jointly fitted cosmological parameters such as the Hubble parameter along with the host galaxy contribution (assuming it to be redshift-independent) from the data itself [15]. The average value of host galaxy contribution from these analyses turns out to be of the order of $50\text{-}100 \text{ pc cm}^{-3}$. Other works [18–20] have used cosmological simulations to compute the host galaxy contribution. These results show that the host galaxy contribution is typically sub-dominant compared to the intergalactic medium. [18] reported that the host galaxy contribution increases with redshift (approximately $\propto (1+z)$ on average) though it depends sensitively on the type of galaxy. Recently, another work [21] studied the DM evolution with redshift using the IllustrisTNG50 simulation [22] and obtained similar results (see Fig. 4 of the reference for comparison) as in [18]. The authors attributed this change to increase in electron density inside the galaxies due to star formation. However, these cosmological simulations lack resolution at smaller scales which can potentially bias their results. A recent work [23] shows that the host galaxy contribution can be dominant or be as important as the intergalactic medium. This work utilised higher resolution FIRE-2 simulations [24] to investigate host DM contribution.

In this work, considering the theoretical uncertainty based on cosmological simulations, we outline a method to empirically constrain the redshift dependence of the mean host galaxy contribution and its redshift evolution, characterized here as a power-law, $\propto (1+z)^\alpha$. The redshift-dependence of host galaxies, if any, can have important consequences for galaxy formation models and will capture cosmological relevant information such as their evolution across cosmic time. Our analysis is based on a few assumptions. We have fixed the halo contribution to a value which has been used in the literature [15, 17]. Subject to these caveats, we find that the current data can exclude $\alpha \gtrsim 2$. In the future, we may rule out (or confirm) $\alpha \gtrsim 1$ which will critically test the results of [18, 21]. We also show that the inferred, best fit value of cosmological parameters such as the baryon density of the Universe and the Hubble parameter are stable to a change in the index α . We organize the paper as follows. In Sec. 2, we discuss the various contribution to the observed DM along with their modelling and introduce our FRB sample. We discuss our procedure for computing likelihood and fitting our model to the data in Sec. 3. In Sec. 4, we discuss our results and end with discussions in Sec. 5.

2 Dispersion measure of FRBs

Radio waves get dispersed due to intervening ionized medium as they travel from the source to us. The observed or total DM can be expressed as,

$$DM_{\text{obs}} = DM_{\text{halo}} + DM_{\text{ISM}} + DM_{\text{IGM}} + \frac{DM_{\text{host}} + DM_{\text{source}}}{1+z} \quad (2.1)$$

where DM_{halo} and DM_{ISM} are the contributions from our Galaxy and the surrounding halo. The IGM contribution comes from the large scale structure of the Universe and depends upon the assumed cosmological model. The host and source terms are contributed by the host galaxy and the immediate surroundings of FRBs respectively, which is redshifted in the observer frame. We have dropped the source term (which for most sources is expected to be subdominant) in this work.

In Table 1, we report the sample of 30 FRBs used in this work along with their redshifts and the observed DM. We have dropped FRBs with exceptionally high DM such as FRB20190520B [25] which is almost certainly dominated by the environment in the near vicinity of the source, which can account also for the persistent emission associated with the source and its anomalously large and fluctuating rotation measure [26]. In Table 1, we give the ISM contribution for the FRBs which depends on their sky location and computed using NE2001 model [27]. These values can be found in the literature such as [6, 8, 28]. We use a value of $DM_{\text{halo}} = 50 \text{ pc cm}^{-3}$ which is typically assumed in the literature [15]. We note that this contribution is uncertain and can have consequences for inferred quantities such as H_0 (Hubble parameter today) as we discuss in §3.1.

FRB	z	DM _{obs}	DM _{ISM}	References
FRB20220319D	0.0112	110.98	133.3	[6]
FRB20180916B	0.0337	348.76	200	[29]
FRB20220207C	0.0430	262.38	79.3	[6]
FRB20211127I	0.0469	234.83	42.5	[30]
FRB20211212A	0.0715	206	27.1	[30]
FRB20220509G	0.0894	269.53	55.2	[6]
FRB20201124A	0.098	413	123	[31]
FRB20220914A	0.1139	631.28	55.2	[6]
FRB20190608B	0.1178	339	37	[15]
FRB20220920A	0.158	314.99	40.3	[6]
FRB20200430A	0.1608	380.25	27	[4]
FRB20121102A	0.19273	557	188	[7]
FRB20191001A	0.234	506.92	44.7	[4]
FRB20190714A	0.2365	504.13	38	[4]
FRB20220825A	0.2414	651.24	79.7	[6]
FRB20191228A	0.2432	297.5	33	[32]
FRB20220307B	0.248	499.27	135.7	[6]
FRB20221012A	0.2846	441.08	54.4	[6]
FRB20190102C	0.2913	363.6	57.3	[15]
FRB20220506D	0.3004	396.97	89.1	[6]
FRB20180924C	0.3214	361.42	40.5	[33]
FRB20180301A	0.3304	536	152	[32]
FRB20200906A	0.3688	577.8	36	[32]
FRB20190611B	0.3778	321.4	57.8	[4]
FRB20181112A	0.4755	589.27	42	[34]
FRB20220310F	0.4779	462.24	45.4	[6]
FRB20190711A	0.5220	593.1	56.4	[4]
FRB20190614D	0.60	959.2	83.5	[35]
FRB20220418A	0.6220	623.25	37.6	[6]
FRB20190523A	0.6600	760.8	37	[36]

Table 1: List of FRBs used in this work along with their associated properties. The dispersion measures are in the units of pc cm^{-3} . We have one burst with $\text{DM}_{\text{ISM}} > \text{DM}_{\text{obs}}$ which is of course non-physical. We note that the estimate of ISM DM contribution assumes the [27] model which uses a smooth distribution of Milky-way electrons as well as large scale fluctuations in their distribution. However, there is some discrepancy in the measurement of distances to high altitude pulsars using this model [37]. This is evident by contrasting this ISM model with the estimates based on the modelling done by, e.g., [38].

2.1 IGM contribution to DM_{obs}

The IGM contribution can be expressed as [16],

$$\langle DM_{\text{IGM}} \rangle (z) = \frac{3cH_0\Omega_{\text{b}0}}{8\pi Gm_{\text{p}}} \int_0^z dz' \frac{(1+z)\xi_e(z)}{[\Omega_{\text{m}0}(1+z')^3 + \Omega_{\Lambda 0}]^{1/2}} \quad (2.2)$$

where $\Omega_{\text{b}0}$, $\Omega_{\text{m}0}$ and $\Omega_{\Lambda 0}$ are the fractional energy density of baryons, matter and dark energy compared to critical energy density today. We assume flat Λ CDM cosmology which ensures $\Omega_{\Lambda 0} = 1 - \Omega_{\text{m}0}$ at the redshifts of interest. We use the best fit value of these parameters as inferred from the CMB (Cosmic Microwave Background) experiments [39]. The expression depends upon the electron fraction $\xi_e(z)$, which in turn depends upon the helium mass fraction (Y). Using $Y \approx 0.25$, we have $\xi_e(z) \approx 0.87$ which holds at $z \lesssim 3$, when helium become fully ionized. We can also rewrite the Hubble parameter as $H_0 = 100h \text{ kms}^{-1}\text{Mpc}^{-1}$ and use the variable h below. From Eq. 2.2, we find that $DM_{\text{IGM}} \propto \Omega_{\text{b}0}h$. Therefore, we can only constrain a degenerate combination of $\Omega_{\text{b}0}h$ from FRB observations. However, CMB measurements can provide $\Omega_{\text{b}0}h^2 = 0.022$ [39] with a tight prior. Therefore, using this prior, we can break this degeneracy and, in that case, DM_{IGM} is inversely proportional to h [30].

While Eq. 2.2 gives the expression for the mean IGM contribution, there can be significant scatter along different lines of sight as matter starts to clump in the late universe. This leads to a variance in the IGM contribution. This variance has been computed in the literature (see, e.g., [40]) using cosmological simulations. It depends sensitively on baryonic physics and can potentially vary among different simulations. Furthermore, the DM_{IGM} may not be normally distributed and can be asymmetric. In this work, we assume the distribution to be Gaussian and use the result of Ziegler et al. (in prep),

$$\frac{\sigma_{\text{IGM}}(z)}{DM_{\text{IGM}}} = 0.316z^{-0.677} \quad (2.3)$$

2.2 Contribution from host galaxy

We assume the host galaxy contribution to be of the form,

$$\langle DM_{\text{host}} \rangle = DM_{\text{host},0}(1+z)^\alpha \quad (2.4)$$

In most of earlier works, α is assumed to be zero. However, the authors of [18] reported an approximate value of $\alpha \approx 1$ from the IllustrisTNG simulation [41]. The number can depend sensitively on the type of galaxy. Recent zoom-in simulations such as [16, 23] show that the host contribution can have a large scatter due to galaxy age, morphology and orientation around a mean value of $\sim 100 \text{ pc cm}^{-3}$ (Fig. 6 of [16] and Fig. 8 of [23]). This scatter in DM_{host} may dominate over the IGM contribution especially at low redshifts. Similar to previous works, we have assumed the scatter of the host to be log-normal. Therefore, we rewrite Eq. 2.4 as,

$$\mu = \mu_0 + \alpha \log(1+z) \quad (2.5)$$

where $\mu = \log \langle DM_{\text{host}} \rangle$ and $\mu_0 = \log(DM_{\text{host},0})$. We assume the scatter in host galaxy contribution to be, $\sigma_{\text{host}}=1$, which was the best fit value obtained in [15].

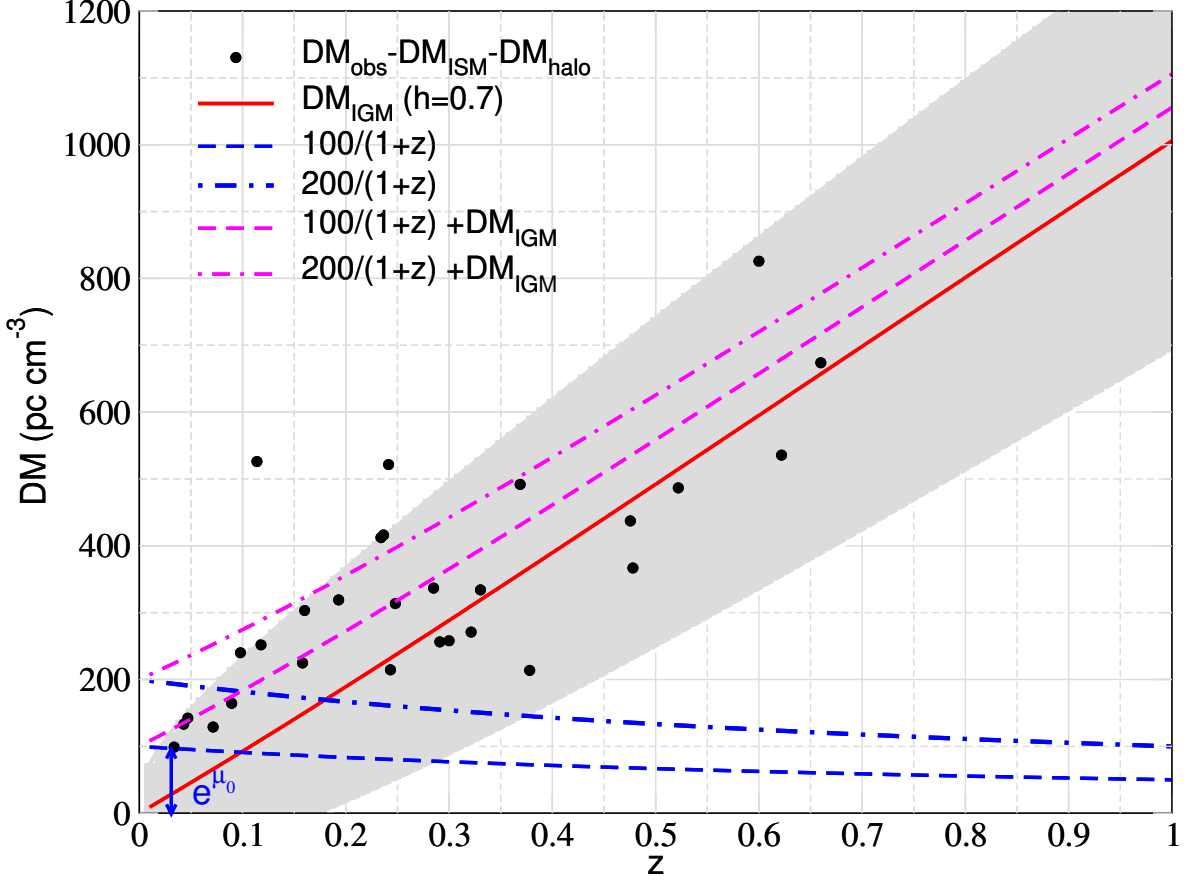


Figure 1: Dispersion measure of our sample of FRBs after subtracting ISM and halo contribution (see §2 for details). We compare it to our fiducial IGM model with $h = 0.7$ and host galaxy contribution with $DM_{\text{host},0} = 100$ and 200 pc cm^{-3} , $\alpha = 0$. The shaded region around the red line shows the $1\text{-}\sigma$ region due to scatter in IGM (Eq. 2.3). At low redshifts, the host contribution dominates over IGM contribution which is shown visually by the blue double-sided arrow.

In Fig. 1, we plot the dispersion measure of our sample of FRBs after subtracting respective ISM and halo contribution. We compare this with a few cases assuming a fiducial cosmology and host galaxy contribution. We clearly see a preference for non-zero host contribution for sources at low redshifts where IGM contribution becomes sub-dominant. While the purpose of the figure is to visually motivate the case for non-zero host contribution, we will fit our model in Eq. 2.5, directly to the data to extract the host galaxy contribution, below.

3 Likelihood analysis

In this work, we use Gaussian likelihood for analysis of data. For an individual FRB, the likelihood of the total observed DM is given by,

$$\mathcal{L}_i(\text{DM}'_i | z_i) = \int_0^{\text{DM}'_i} p_{\text{host}}(\text{DM}_{\text{host}} | \mu, \sigma_{\text{host}}) p_{\text{IGM}}(\text{DM}'_i - \text{DM}_{\text{host}}, z_i) d\text{DM}_{\text{host}}, \quad (3.1)$$

where,

$$p_{\text{host}} = \frac{1}{\sqrt{2\pi\sigma_{\text{host}}^2} \text{DM}_{\text{host}}} \exp\left(-\frac{(\log(\text{DM}_{\text{host}}) - \mu)^2}{2\sigma_{\text{host}}^2}\right), \quad (3.2)$$

and,

$$p_{\text{IGM}} = \frac{1}{\sqrt{2\pi\sigma_{\text{IGM}}^2}} \exp\left(-\frac{(\text{DM}'_i - \frac{\text{DM}_{\text{host}}}{1+z_i} - \langle \text{DM}_{\text{IGM}} \rangle)^2}{2\sigma_{\text{IGM}}^2}\right), \quad (3.3)$$

with $\text{DM}'_i = \text{DM}_{\text{obs}} - \text{DM}_{\text{i,ISM}} - \text{DM}_{\text{halo}}$. Since all FRBs are independent, the joint likelihood is given by the individual likelihood products,

$$\mathcal{L}_{\text{tot}} = \prod_i^N \mathcal{L}_i, \quad (3.4)$$

where N is the number of FRBs in the sample which is 30 in our case. We use MCMC (Markov Chain Monte Carlo) sampling to scan over the parameter space. Up to this point, the free parameters, in this work, are h , μ_0 and α . We remind the reader that the halo contribution is also uncertain which can be degenerate with other terms such as the IGM contribution. Therefore, we study the degeneracy between DM_{halo} and h first.

3.1 Degeneracy between halo contribution and h

We scan over DM_{halo} and h in our likelihood analysis keeping $\alpha = 0$ and μ_0 to its reference value which is 100 pc cm^{-3} . We show the 2D posterior or correlation between the two parameters in Fig. 2. As we increase DM_{halo} , the contribution from the IGM has to decrease in order to compensate. As we have shown previously, $\text{DM}_{\text{IGM}} \propto h^{-1}$, the value of h has to increase. This explains the behaviour seen in Fig. 2. Therefore, one needs to vary both DM_{halo} and h simultaneously for consistency. This increases the dimensionality of the problem. In the literature, various authors have fixed DM_{halo} and scanned over h in order to infer its value from FRB data [15, 17]. This potentially leads to biased results as Fig. 2 shows. This can be a problem once we have a large number of FRBs such that the error bar on the inferred value of h shrinks appreciably. For simplicity, we have fixed both DM_{halo} and h to their assumed fiducial values of 50 pc cm^{-3} and 0.7 respectively. Therefore, in §4, we have two remaining free parameters μ_0 and α which we vary to fit the data.

4 Results

In Fig. 3 and 4, we plot the main results of this work. We show the 1D posterior on each parameter after marginalizing over the other parameters. In Fig. 3, we impose the criteria that $\alpha > 0$. This

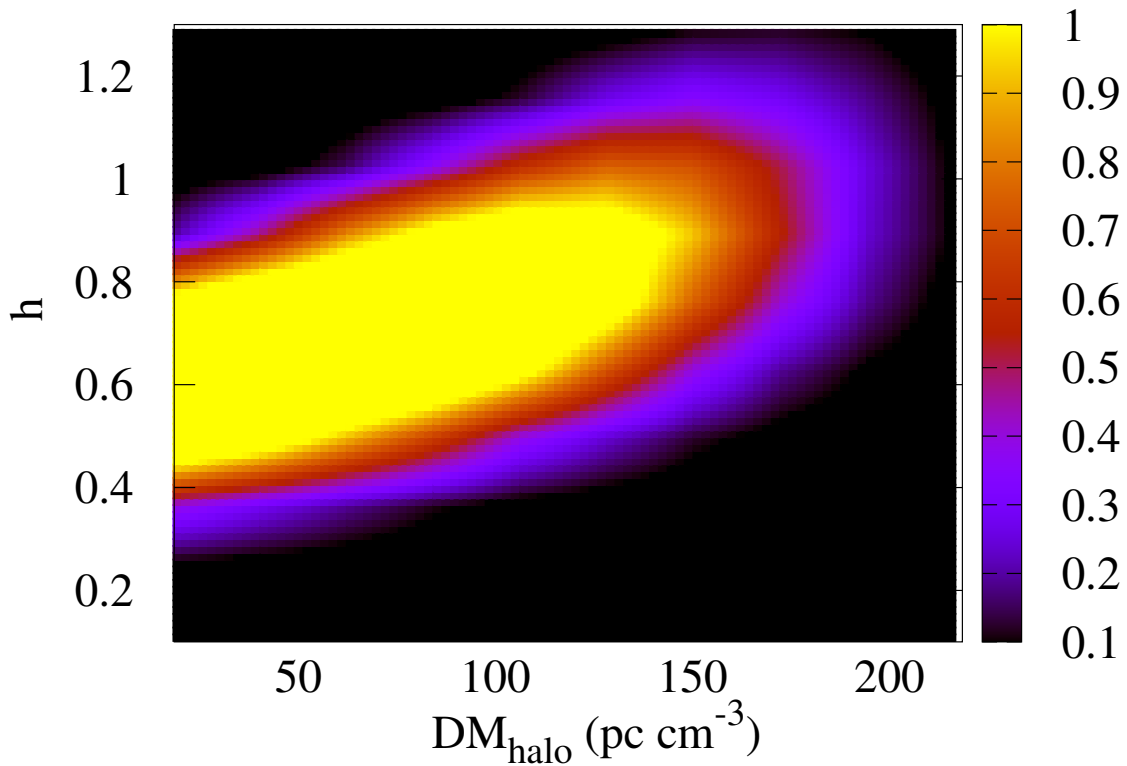


Figure 2: Joint probability $\frac{dP}{d(DM_{\text{halo}}h)} \times 100$ where the factor 100 is chosen for better normalization and plotting efficiency.

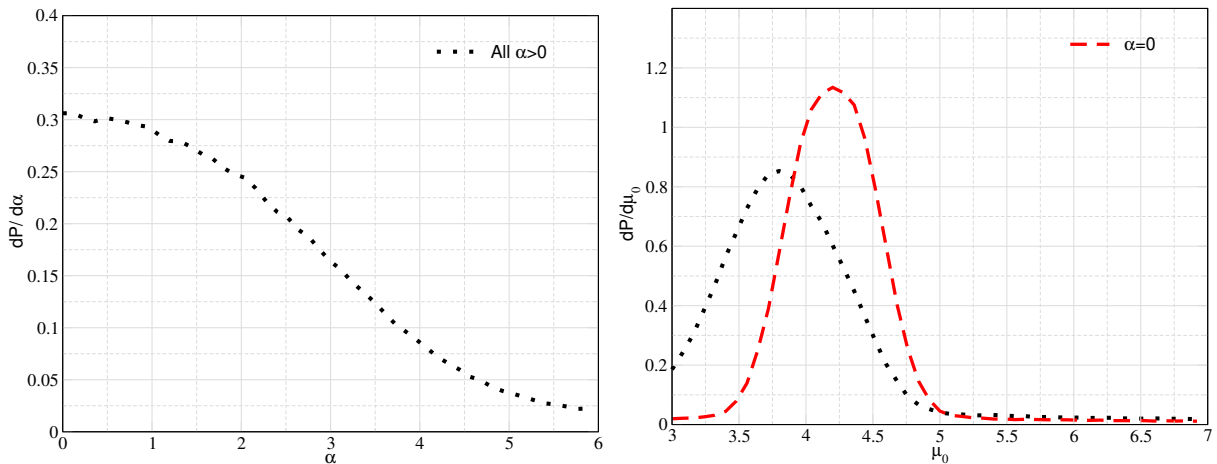


Figure 3: Constraints, in terms of the associated probability distribution function, on α and μ_0 obtained by putting a prior on $\alpha > 0$. For our fiducial case with $\alpha = 0$, the best fit value of $\mu_0 \approx 4.3$ which amounts to $DM_{\text{host},0} \approx 80 \text{ pc cm}^{-3}$.

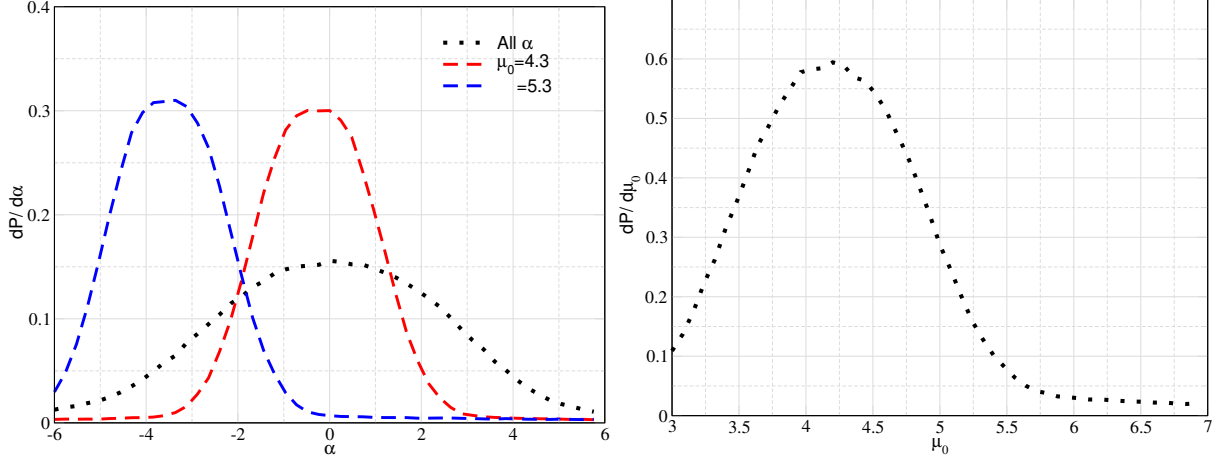


Figure 4: Constraints on α and μ_0 by allowing α to have either sign. We consider two cases with fixed μ_0 . One with with best fit value of $\mu_0 = 4.3$ which results in $DM_{\text{host},0} \approx 80 \text{ pc cm}^{-3}$ and the second one such that $e^{\mu_0} = 200 \text{ pc cm}^{-3}$.

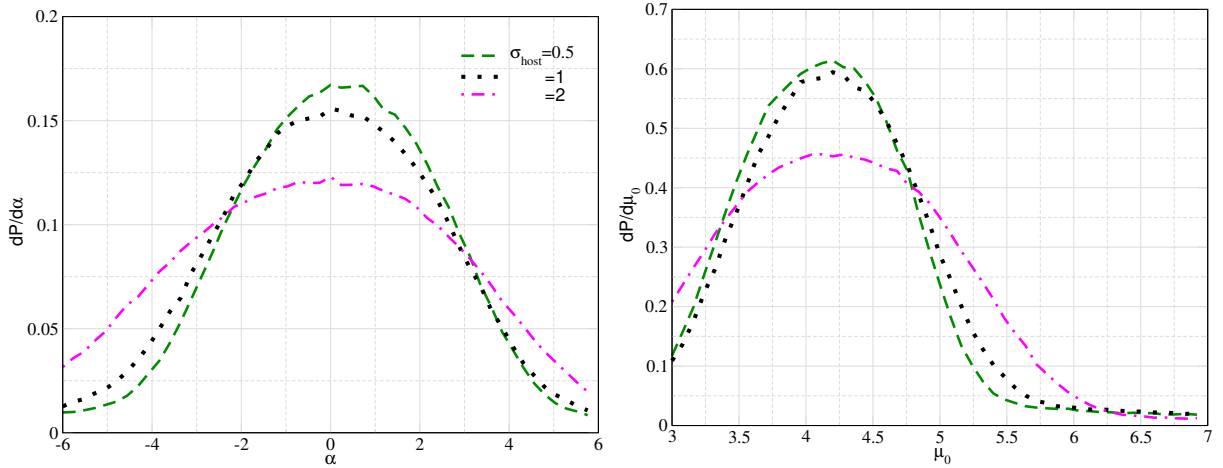


Figure 5: Constraints on α and μ_0 by varying σ_{host} .

is motivated from the fact that at higher redshifts, the universe is denser. Therefore, due to higher density, the host contribution should increase with redshift (see e.g. estimates by [16] of DM_{host} at high z based on zoom-in FIRE simulations). We find that the current data can already put interesting constraints on α . We find that $\alpha = 0$ is preferred over higher values. For our fiducial case with $\alpha = 0$, the best fit value of $\mu_0 \approx 4.3$ or $DM_{\text{host},0} \approx 80 \text{ pc cm}^{-3}$. For $\alpha > 0$ case, the best fit value of $\mu_0 \approx 4$ or $DM_{\text{host},0} \approx 50 \text{ pc cm}^{-3}$ which is a bit smaller but is similar to the results obtained in [15].

As a next step, we do not impose the positivity constraint on α and allow it to have both signs. The results are plotted in Fig. 4. In such a case, $\alpha \approx 0$ is still preferred. The best fit value of μ_0 remains about 4-4.5. We find that a high value of α (with either sign) is strongly disfavoured. In the future, as our sample size increases, the upper limit will also reduce approximately as \sqrt{N} where N

is the number of FRBs in the sample. Thereby, by increasing our sample size, we may rule out $\alpha \gtrsim 1$ at high statistical significance and, therefore, we should be in a position to test the results of [18, 21]. Even without additional data, if we impose a strong prior on μ_0 , we can already obtain very strong constraints. As shown in Fig. 4, by fixing μ_0 to its best fit value of 4.3, $|\alpha| > 2$ can already be seen as strongly unfavourable. By fixing μ_0 to higher values, there is a strong preference for negative α which is expected because of the degeneracy (Eq. 2.4). As FRBs are detected at higher and higher redshifts, the constraints should tighten as the degeneracy between α and μ_0 will be broken increasingly more effectively.

In Fig. 5, we vary the standard deviation of DM_{host} , σ_{host} . Qualitatively, the constraints on α do not change drastically. However, the posterior distribution becomes flatter for higher σ_{host} . In the future, one can try to infer σ_{host} from the data itself. For a small sample size as considered in this work, a larger number of parameters can lead to significant degeneracies. However, once we have a bigger sample, we may be able to break the degeneracies and infer these parameters consistently from the data.

4.1 Degeneracy between inferred $\Omega_{\text{b}0}h$ and α

Next, we consider the degeneracy between the inferred cosmological parameters $\Omega_{\text{b}0}h$ and α . We use Eq. 2.2 to compute the DM_{IGM} contribution and do not use CMB prior to eliminate $\Omega_{\text{b}0}$. We also fix DM_{halo} to its assumed value and μ_0 as denoted in Fig. 6. The best fit value of $\Omega_{\text{b}0}h$ does not shift much and α roughly has a similar distribution to that shown in Fig. 4. This is expected since $\Omega_{\text{b}0}h$ is just a constant while α controls the redshift dependence of the host galaxy DM contribution. Therefore, there isn't a significant correlation between the two. However, there is a non-negligible $\Omega_{\text{b}0}h$ distribution tail at both ends. This small degeneracy can be broken as more FRBs are detected and particularly, ones at higher and higher redshifts.

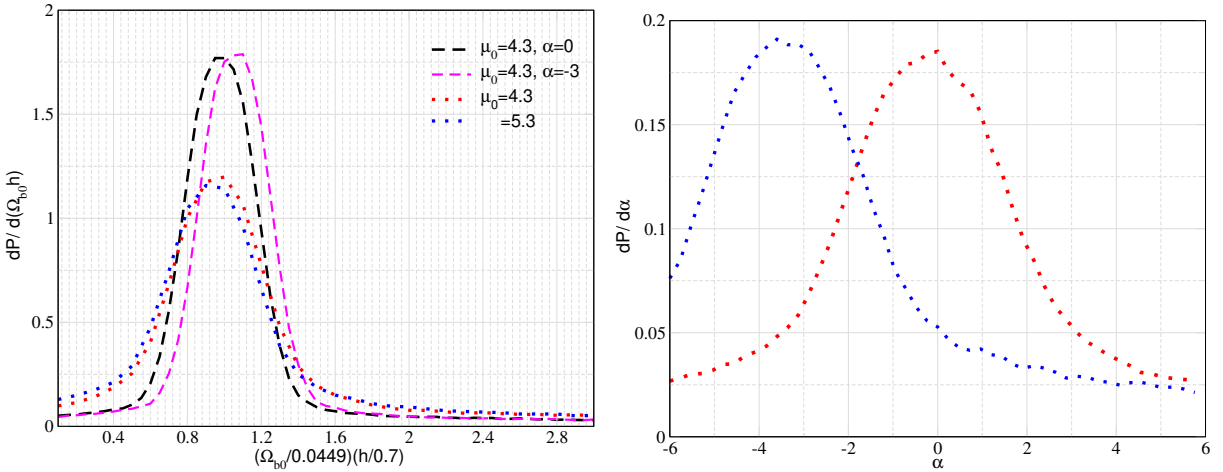


Figure 6: Constraints on $\Omega_{\text{b}0}h$ and α by fitting these two parameters to data while keeping μ_0 fixed to its prescribed value. We derive constraints on $\Omega_{\text{b}0}h$ for two cases, where we fix α (dashed lines) as well as μ_0 and two cases (dotted lines) where we fix μ_0 while marginalizing over α .

5 Discussion and conclusions

We have constrained the redshift dependence of host galaxy dispersion measures assuming that the dependence can be parameterized by a power law in $(1+z)$. We considered a sample of 30 FRBs with redshifts of up to 0.7 and fitted the observed DM with the combination of host galaxy, IGM, Milky way and its halo contribution. Using the current data, the parameter space with $\alpha \approx 0$ is preferred. These results can inform us about galaxy formation physics and how the host DM depends on it. There is a significant degeneracy between α and μ_0 which compensate each other for the host galaxy contribution. We expect this degeneracy to be broken as we detect FRBs at higher redshifts. The host DM can also have significant contributions from the circumgalactic medium. To a first approximation, this can be absorbed into our effective definition of DM_{host} (although it is unclear if the two terms should evolve with redshift in a similar way). Additionally, a foreground galaxy can contribute significantly to the DM of a background galaxy [42], however, the fraction of such foreground galaxies appears to be $\lesssim 5\%$ (Fig. 1 of [42]). Therefore, we do not expect significant systematics to be introduced by ignoring these foregrounds. In the future, we may isolate a statistically significant sample of bursts whose lines of sight go through such foreground galaxies and repeat our analysis. These may have implications for our understanding on the distribution of diffuse gas around galaxies.

As a second step, we fit the data with varying $\Omega_{\text{b}0}h$ and α for a few representative values of μ_0 . We find that the best fit value of $\Omega_{\text{b}0}h$ is stable to changes in α , though, it adds a non-negligible amount of scatter around the best-fit $\Omega_{\text{b}0}h$ value. We expect these degeneracies to be broken significantly with a bigger sample and more detected FRBs from higher redshifts. This is because the power law contribution $(1+z)^\alpha$ is sensitive to the available values of z . For the sample considered in this work, most of the FRBs are at $z \lesssim 0.4$ which makes the $(1+z)^\alpha$ term less sensitive to changes in redshift within the range stated above.

Our results rely on a few assumptions. We have assumed knowledge of the scatter in the host galaxy DMs, σ_{host} . Alternatively, we may try to infer this directly from the data. We also point out that our inference of cosmological parameters such as α and $\Omega_{\text{b}0}h$ depends sensitively on how we partition the observed DM to its various constituents. As an example, we show how the inferred value of h changes as we vary DM_{halo} (Fig. 2). Ideally, we would want to fit all the unknown parameters to the data and obtain their posterior distribution. In the future, a large sample with a significant number of FRBs at $z \gtrsim 1$ will propel us towards that goal. Most detected FRBs, to date, do not have an identified redshift. This larger sample of FRBs has not been used in the present analysis. However, correlating this larger FRB sample with galaxy sky maps, can provide useful statistical constraints on the typical redshift of FRBs [43] even when redshifts of individual bursts remains undetermined and this information, in turn, can be fed back into the analysis presented in this work, to improve its statistical power.

Acknowledgements

SKA is supported by the ARCO fellowship. PB is supported by a grant (no. 2020747) from the United States-Israel Binational Science Foundation (BSF), Jerusalem, Israel, by a grant (no. 1649/23) from the Israel Science Foundation and by a grant (no. 80NSSC 24K0770) from the NASA astrophysics theory program.

References

- [1] D. R. Lorimer, M. Bailes, M. A. McLaughlin, D. J. Narkevic, and F. Crawford. A Bright Millisecond Radio Burst of Extragalactic Origin. *Science*, 318(5851):777, November 2007. [arXiv:0709.4301](#), [\[DOI\]](#), [\[ADS\]](#).
- [2] E. Petroff, E. D. Barr, A. Jameson, E. F. Keane, M. Bailes, M. Kramer, V. Morello, D. Tabbara, and W. van Straten. FRBCAT: The Fast Radio Burst Catalogue. *Publications of the Astronomical Society of Australia*, 33:e045, September 2016. [arXiv:1601.03547](#), [\[DOI\]](#), [\[ADS\]](#).
- [3] CHIME/FRB Collaboration, M. Amiri, K. Bandura, M. Bhardwaj, P. Boubel, M. M. Boyce, P. J. Boyle, C. Brar, M. Burhanpurkar, P. Chawla, J. F. Cliche, D. Cubranic, M. Deng, N. Denman, M. Dobbs, M. Fandino, E. Fonseca, B. M. Gaensler, A. J. Gilbert, U. Giri, D. C. Good, M. Halpern, D. Hanna, A. S. Hill, G. Hinshaw, C. Höfer, A. Josephy, V. M. Kaspi, T. L. Landecker, D. A. Lang, K. W. Masui, R. Mckinven, J. Mena-Parra, M. Merryfield, N. Milutinovic, C. Moatti, A. Naidu, L. B. Newburgh, C. Ng, C. Patel, U. Pen, T. Pinsonneault-Marotte, Z. Pleunis, M. Rafiei-Ravandi, S. M. Ransom, A. Renard, P. Scholz, J. R. Shaw, S. R. Siegel, K. M. Smith, I. H. Stairs, S. P. Tendulkar, I. Tretyakov, K. Vanderlinde, and P. Yadav. Observations of fast radio bursts at frequencies down to 400 megahertz. *Nature*, 566(7743):230–234, January 2019. [arXiv:1901.04524](#), [\[DOI\]](#), [\[ADS\]](#).
- [4] Kasper E. Heintz, J. Xavier Prochaska, Sunil Simha, Emma Platts, Wen-fai Fong, Nicolas Tejos, Stuart D. Ryder, Kshitij Aggerwal, Shivani Bhandari, Cherie K. Day, Adam T. Deller, Charles D. Kilpatrick, Casey J. Law, Jean-Pierre Macquart, Alexandra Mannings, Lachlan J. Marnoch, Elaine M. Sadler, and Ryan M. Shannon. Host Galaxy Properties and Offset Distributions of Fast Radio Bursts: Implications for Their Progenitors. *ApJ*, 903(2):152, November 2020. [arXiv:2009.10747](#), [\[DOI\]](#), [\[ADS\]](#).
- [5] C. W. James, E. M. Ghosh, J. X. Prochaska, K. W. Bannister, S. Bhandari, C. K. Day, A. T. Deller, M. Glowacki, A. C. Gordon, K. E. Heintz, L. Marnoch, S. D. Ryder, D. R. Scott, R. M. Shannon, and N. Tejos. A measurement of Hubble’s Constant using Fast Radio Bursts. *MNRAS*, 516(4):4862–4881, November 2022. [arXiv:2208.00819](#), [\[DOI\]](#), [\[ADS\]](#).
- [6] Casey J. Law, Kritti Sharma, Vikram Ravi, Ge Chen, Morgan Catha, Liam Connor, Jakob T. Faber, Gregg Hallinan, Charlie Harnach, Greg Hellbourg, Rick Hobbs, David Hodge, Mark Hodges, James W. Lamb, Paul Rasmussen, Myles B. Sherman, Jun Shi, Dana Simard, Reynier Squillace, Sander Weinreb, David P. Woody, and Nitika Yadlapalli Yurk. Deep Synoptic Array Science: First FRB and Host Galaxy Catalog. *ApJ*, 967(1):29, May 2024. [arXiv:2307.03344](#), [\[DOI\]](#), [\[ADS\]](#).
- [7] S. Chatterjee, C. J. Law, R. S. Wharton, S. Burke-Spolaor, J. W. T. Hessels, G. C. Bower, J. M. Cordes, S. P. Tendulkar, C. G. Bassa, P. Demorest, B. J. Butler, A. Seymour, P. Scholz, M. W. Abruzzo, S. Bogdanov, V. M. Kaspi, A. Keimpema, T. J. W. Lazio, B. Marcote, M. A. McLaughlin, Z. Paragi, S. M. Ransom, M. Rupen, L. G. Spitler, and H. J. van Langevelde. A direct localization of a fast radio burst and its host. *Nature*, 541(7635):58–61, January 2017. [arXiv:1701.01098](#), [\[DOI\]](#), [\[ADS\]](#).

- [8] Bing Zhang. The physics of fast radio bursts. *Reviews of Modern Physics*, 95(3):035005, July 2023. [arXiv:2212.03972](#), [\[DOI\]](#), [\[ADS\]](#).
- [9] L. G. Spitler, P. Scholz, J. W. T. Hessels, S. Bogdanov, A. Brazier, F. Camilo, S. Chatterjee, J. M. Cordes, F. Crawford, J. Deneva, R. D. Ferdman, P. C. C. Freire, V. M. Kaspi, P. Lazarus, R. Lynch, E. C. Madsen, M. A. McLaughlin, C. Patel, S. M. Ransom, A. Seymour, I. H. Stairs, B. W. Stappers, J. van Leeuwen, and W. W. Zhu. A repeating fast radio burst. *Nature*, 531(7593):202–205, March 2016. [arXiv:1603.00581](#), [\[DOI\]](#), [\[ADS\]](#).
- [10] E. Petroff, J. W. T. Hessels, and D. R. Lorimer. Fast radio bursts at the dawn of the 2020s. *The Astronomy and Astrophysics Review*, 30(1):2, December 2022. [arXiv:2107.10113](#), [\[DOI\]](#), [\[ADS\]](#).
- [11] Matthew McQuinn. Locating the “Missing” Baryons with Extragalactic Dispersion Measure Estimates. *ApJL*, 780(2):L33, January 2014. [arXiv:1309.4451](#), [\[DOI\]](#), [\[ADS\]](#).
- [12] David Eichler. Nanolensed Fast Radio Bursts. *ApJ*, 850(2):159, December 2017. [arXiv:1711.04764](#), [\[DOI\]](#), [\[ADS\]](#).
- [13] Adi Zitrin and David Eichler. Observing Cosmological Processes in Real Time with Repeating Fast Radio Bursts. *ApJ*, 866(2):101, October 2018. [arXiv:1807.03287](#), [\[DOI\]](#), [\[ADS\]](#).
- [14] Zheng-Xiang Li, He Gao, Xu-Heng Ding, Guo-Jian Wang, and Bing Zhang. Strongly lensed repeating fast radio bursts as precision probes of the universe. *Nature Communications*, 9:3833, September 2018. [arXiv:1708.06357](#), [\[DOI\]](#), [\[ADS\]](#).
- [15] J. P. Macquart, J. X. Prochaska, M. McQuinn, K. W. Bannister, S. Bhandari, C. K. Day, A. T. Deller, R. D. Ekers, C. W. James, L. Marnoch, S. Osłowski, C. Phillips, S. D. Ryder, D. R. Scott, R. M. Shannon, and N. Tejos. A census of baryons in the Universe from localized fast radio bursts. *Nature*, 581(7809):391–395, May 2020. [arXiv:2005.13161](#), [\[DOI\]](#), [\[ADS\]](#).
- [16] Paz Beniamini, Pawan Kumar, Xiangcheng Ma, and Eliot Quataert. Exploring the epoch of hydrogen reionization using FRBs. *MNRAS*, 502(4):5134–5146, April 2021. [arXiv:2011.11643](#), [\[DOI\]](#), [\[ADS\]](#).
- [17] Steffen Hagstotz, Robert Reischke, and Robert Lilow. A new measurement of the Hubble constant using fast radio bursts. *MNRAS*, 511(1):662–667, March 2022. [arXiv:2104.04538](#), [\[DOI\]](#), [\[ADS\]](#).
- [18] G. Q. Zhang, Hai Yu, J. H. He, and F. Y. Wang. Dispersion Measures of Fast Radio Burst Host Galaxies Derived from IllustrisTNG Simulation. *ApJ*, 900(2):170, September 2020. [arXiv:2007.13935](#), [\[DOI\]](#), [\[ADS\]](#).
- [19] Alexander Theis, Steffen Hagstotz, Robert Reischke, and Jochen Weller. Galaxy dispersion measured by Fast Radio Bursts as a probe of baryonic feedback models. *arXiv e-prints*, page arXiv:2403.08611, March 2024. [arXiv:2403.08611](#), [\[DOI\]](#), [\[ADS\]](#).
- [20] Jian-Feng Mo, Weishan Zhu, Yang Wang, Lin Tang, and Long-Long Feng. The dispersion measure of Fast Radio Bursts host galaxies: estimation from cosmological simulations. *MNRAS*, 518(1):539–561, January 2023. [arXiv:2210.14052](#), [\[DOI\]](#), [\[ADS\]](#).
- [21] Tímea Orsolya Kovacs, Sui Ann Mao, Aritra Basu, Yik Ki Ma, Laura G. Spitler, and Charles R. H. Walker. The dispersion measure and rotation measure from fast radio burst host galaxies based on the IllustrisTNG50 simulation. *arXiv e-prints*, page arXiv:2407.16748, July 2024. [arXiv:2407.16748](#), [\[ADS\]](#).

- [22] Annalisa Pillepich, Dylan Nelson, Volker Springel, Rüdiger Pakmor, Paul Torrey, Rainer Weinberger, Mark Vogelsberger, Federico Marinacci, Shy Genel, Arjen van der Wel, and Lars Hernquist. First results from the TNG50 simulation: the evolution of stellar and gaseous discs across cosmic time. *MNRAS*, 490(3):3196–3233, December 2019. [arXiv:1902.05553](#), [DOI], [ADS].
- [23] Matthew E. Orr, Blakesley Burkhart, Wenbin Lu, Sam B. Ponnada, and Cameron B. Hummels. Objects May Be Closer Than They Appear: Significant Host Galaxy Dispersion Measures of Fast Radio Bursts in Zoom-in Simulations. *arXiv e-prints*, page arXiv:2406.03523, June 2024. [arXiv:2406.03523](#), [DOI], [ADS].
- [24] Philip F. Hopkins, Andrew Wetzel, Dušan Kereš, Claude-André Faucher-Giguère, Eliot Quataert, Michael Boylan-Kolchin, Norman Murray, Christopher C. Hayward, Shea Garrison-Kimmel, Cameron Hummels, Robert Feldmann, Paul Torrey, Xiangcheng Ma, Daniel Anglés-Alcázar, Kung-Yi Su, Matthew Orr, Denise Schmitz, Ivanna Escala, Robyn Sanderson, Michael Y. Grudić, Zachary Hafen, Ji-Hoon Kim, Alex Fitts, James S. Bullock, Coral Wheeler, T. K. Chan, Oliver D. Elbert, and Desika Narayanan. FIRE-2 simulations: physics versus numerics in galaxy formation. *MNRAS*, 480(1):800–863, October 2018. [arXiv:1702.06148](#), [DOI], [ADS].
- [25] C. H. Niu, K. Aggarwal, D. Li, X. Zhang, S. Chatterjee, C. W. Tsai, W. Yu, C. J. Law, S. Burke-Spolaor, J. M. Cordes, Y. K. Zhang, S. K. Ocker, J. M. Yao, P. Wang, Y. Feng, Y. Niino, C. Bochenek, M. Cruces, L. Connor, J. A. Jiang, S. Dai, R. Luo, G. D. Li, C. C. Miao, J. R. Niu, R. Anna-Thomas, J. Sydnor, D. Stern, W. Y. Wang, M. Yuan, Y. L. Yue, D. J. Zhou, Z. Yan, W. W. Zhu, and B. Zhang. A repeating fast radio burst associated with a persistent radio source. *Nature*, 606(7916):873–877, June 2022. [arXiv:2110.07418](#), [DOI], [ADS].
- [26] Reshma Anna-Thomas, Liam Connor, Shi Dai, Yi Feng, Sarah Burke-Spolaor, Paz Beniamini, Yuan-Pei Yang, Yong-Kun Zhang, Kshitij Aggarwal, Casey J. Law, Di Li, Chenhui Niu, Shami Chatterjee, Marilyn Cruces, Ran Duan, Miroslav D. Filipovic, George Hobbs, Ryan S. Lynch, Chenchen Miao, Jiarui Niu, Stella K. Ocker, Chao-Wei Tsai, Pei Wang, Mengyao Xue, Ju-Mei Yao, Wenfei Yu, Bing Zhang, Lei Zhang, Shiqiang Zhu, and Weiwei Zhu. Magnetic field reversal in the turbulent environment around a repeating fast radio burst. *Science*, 380(6645):599–603, May 2023. [arXiv:2202.11112](#), [DOI], [ADS].
- [27] J. M. Cordes and T. J. W. Lazio. NE2001.I. A New Model for the Galactic Distribution of Free Electrons and its Fluctuations. *arXiv e-prints*, page 0207156, July 2002. [arXiv:0207156](#), [DOI], [ADS].
- [28] Jun-Jie Wei and Fulvio Melia. Investigating Cosmological Models and the Hubble Tension Using Localized Fast Radio Bursts. *ApJ*, 955(2):101, October 2023. [arXiv:2308.05918](#), [DOI], [ADS].
- [29] B. Marcote, K. Nimmo, J. W. T. Hessels, S. P. Tendulkar, C. G. Bassa, Z. Paragi, A. Keimpema, M. Bhardwaj, R. Karuppusamy, V. M. Kaspi, C. J. Law, D. Michilli, K. Aggarwal, B. Andersen, A. M. Archibald, K. Bandura, G. C. Bower, P. J. Boyle, C. Brar, S. Burke-Spolaor, B. J. Butler, T. Cassanelli, P. Chawla, P. Demorest, M. Dobbs, E. Fonseca, U. Giri, D. C. Good, K. Gourdji, A. Josephy, A. Yu. Kirichenko, F. Kirsten, T. L. Landecker, D. Lang, T. J. W. Lazio, D. Z. Li, H. H. Lin, J. D. Linfood, K. Masui, J. Mena-Parra, A. Naidu, C. Ng, C. Patel, U. L. Pen, Z. Pleunis, M. Rafiei-Ravandi, M. Rahman, A. Renard, P. Scholz, S. R. Siegel, K. M. Smith, I. H. Stairs, K. Vanderlinde, and A. V. Zwaniga. A repeating fast radio burst source localized to a nearby spiral galaxy. *Nature*, 577(7789):190–194, January 2020. [arXiv:2001.02222](#), [DOI], [ADS].
- [30] C. W. James, E. M. Ghosh, J. X. Prochaska, K. W. Bannister, S. Bhandari, C. K. Day, A. T. Deller, M. Glowacki, A. C. Gordon, K. E. Heintz, L. Marnoch, S. D. Ryder, D. R. Scott, R. M. Shannon, and

- N. Tejos. A measurement of Hubble’s Constant using Fast Radio Bursts. *MNRAS*, 516(4):4862–4881, November 2022. [arXiv:2208.00819](#), [\[DOI\]](#), [\[ADS\]](#).
- [31] Vikram Ravi, Casey J. Law, Dongzi Li, Kshitij Aggarwal, Mohit Bhardwaj, Sarah Burke-Spolaor, Liam Connor, T. Joseph W. Lazio, Dana Simard, Jean Somalwar, and Shriharsh P. Tendulkar. The host galaxy and persistent radio counterpart of FRB 20201124A. *MNRAS*, 513(1):982–990, June 2022. [arXiv:2106.09710](#), [\[DOI\]](#), [\[ADS\]](#).
- [32] Shivani Bhandari, Kasper E. Heintz, Kshitij Aggarwal, Lachlan Marnoch, Cherie K. Day, Jessica Sydnor, Sarah Burke-Spolaor, Casey J. Law, J. Xavier Prochaska, Nicolas Tejos, Keith W. Bannister, Bryan J. Butler, Adam T. Deller, R. D. Ekers, Chris Flynn, Wen-fai Fong, Clancy W. James, T. Joseph W. Lazio, Rui Luo, Elizabeth K. Mahony, Stuart D. Ryder, Elaine M. Sadler, Ryan M. Shannon, JinLin Han, Kejia Lee, and Bing Zhang. Characterizing the Fast Radio Burst Host Galaxy Population and its Connection to Transients in the Local and Extragalactic Universe. *AJ*, 163(2):69, February 2022. [arXiv:2108.01282](#), [\[DOI\]](#), [\[ADS\]](#).
- [33] K. W. Bannister, A. T. Deller, C. Phillips, J. P. Macquart, J. X. Prochaska, N. Tejos, S. D. Ryder, E. M. Sadler, R. M. Shannon, S. Simha, C. K. Day, M. McQuinn, F. O. North-Hickey, S. Bhandari, W. R. Arcus, V. N. Bennert, J. Burchett, M. Bouwhuis, R. Dodson, R. D. Ekers, W. Farah, C. Flynn, C. W. James, M. Kerr, E. Lenc, E. K. Mahony, J. O’Meara, S. Osłowski, H. Qiu, T. Treu, V. U, T. J. Bateman, D. C. J. Bock, R. J. Bolton, A. Brown, J. D. Bunton, A. P. Chippendale, F. R. Cooray, T. Cornwell, N. Gupta, D. B. Hayman, M. Kesteven, B. S. Koribalski, A. MacLeod, N. M. McClure-Griffiths, S. Neuhold, R. P. Norris, M. A. Pilawa, R. Y. Qiao, J. Reynolds, D. N. Roxby, T. W. Shimwell, M. A. Voronkov, and C. D. Wilson. A single fast radio burst localized to a massive galaxy at cosmological distance. *Science*, 365(6453):565–570, August 2019. [arXiv:1906.11476](#), [\[DOI\]](#), [\[ADS\]](#).
- [34] J. Xavier Prochaska, Jean-Pierre Macquart, Matthew McQuinn, Sunil Simha, Ryan M. Shannon, Cherie K. Day, Lachlan Marnoch, Stuart Ryder, Adam Deller, Keith W. Bannister, Shivani Bhandari, Rongmon Bordoloi, John Bunton, Hyerin Cho, Chris Flynn, Elizabeth K. Mahony, Chris Phillips, Hao Qiu, and Nicolas Tejos. The low density and magnetization of a massive galaxy halo exposed by a fast radio burst. *Science*, 366(6462):231–234, October 2019. [arXiv:1909.11681](#), [\[DOI\]](#), [\[ADS\]](#).
- [35] Casey J. Law, Bryan J. Butler, J. Xavier Prochaska, Barak Zackay, Sarah Burke-Spolaor, Alexandra Mannings, Nicolas Tejos, Alexander Josephy, Bridget Andersen, Pragma Chawla, Kasper E. Heintz, Kshitij Aggarwal, Geoffrey C. Bower, Paul B. Demorest, Charles D. Kilpatrick, T. Joseph W. Lazio, Justin Linford, Ryan Mckinven, Shriharsh Tendulkar, and Sunil Simha. A Distant Fast Radio Burst Associated with Its Host Galaxy by the Very Large Array. *ApJ*, 899(2):161, August 2020. [arXiv:2007.02155](#), [\[DOI\]](#), [\[ADS\]](#).
- [36] V. Ravi, M. Catha, L. D’Addario, S. G. Djorgovski, G. Hallinan, R. Hobbs, J. Kocz, S. R. Kulkarni, J. Shi, H. K. Vedantham, S. Weinreb, and D. P. Woody. A fast radio burst localized to a massive galaxy. *Nature*, 572(7769):352–354, August 2019. [arXiv:1907.01542](#), [\[DOI\]](#), [\[ADS\]](#).
- [37] S. Chatterjee, W. F. Brisken, W. H. T. Vlemmings, W. M. Goss, T. J. W. Lazio, J. M. Cordes, S. E. Thorsett, E. B. Fomalont, A. G. Lyne, and M. Kramer. Precision Astrometry with the Very Long Baseline Array: Parallaxes and Proper Motions for 14 Pulsars. *ApJ*, 698(1):250–265, June 2009. [arXiv:0901.1436](#), [\[DOI\]](#), [\[ADS\]](#).
- [38] J. M. Yao, R. N. Manchester, and N. Wang. A New Electron-density Model for Estimation of Pulsar and FRB Distances. *ApJ*, 835(1):29, January 2017. [arXiv:1610.09448](#), [\[DOI\]](#), [\[ADS\]](#).

- [39] Planck Collaboration. Planck 2018 results. VI. Cosmological parameters. *A&A*, 641:A6, September 2020. [arXiv:1807.06209](#), [\[DOI\]](#), [\[ADS\]](#).
- [40] M. Jaroszynski. Fast radio bursts and cosmological tests. *MNRAS*, 484(2):1637–1644, April 2019. [arXiv:1812.11936](#), [\[DOI\]](#), [\[ADS\]](#).
- [41] Dylan Nelson, Volker Springel, Annalisa Pillepich, Vicente Rodriguez-Gomez, Paul Torrey, Shy Genel, Mark Vogelsberger, Ruediger Pakmor, Federico Marinacci, Rainer Weinberger, Luke Kelley, Mark Lovell, Benedikt Diemer, and Lars Hernquist. The IllustrisTNG simulations: public data release. *Computational Astrophysics and Cosmology*, 6(1):2, May 2019. [arXiv:1812.05609](#), [\[DOI\]](#), [\[ADS\]](#).
- [42] Liam Connor and Vikram Ravi. The observed impact of galaxy halo gas on fast radio bursts. *Nature Astronomy*, 6:1035–1042, July 2022. [arXiv:2107.13692](#), [\[DOI\]](#), [\[ADS\]](#).
- [43] Masoud Rafei-Ravandi, Kendrick M. Smith, Dongzi Li, Kiyoshi W. Masui, Alexander Josephy, Matt Dobbs, Dustin Lang, Mohit Bhardwaj, Chitrang Patel, Kevin Bandura, Sabrina Berger, P. J. Boyle, Charanjot Brar, Daniela Breitman, Tomas Cassanelli, Pragya Chawla, Fengqiu Adam Dong, Emmanuel Fonseca, B. M. Gaensler, Utkarsh Giri, Deborah C. Good, Mark Halpern, Jane Kaczmarek, Victoria M. Kaspi, Calvin Leung, Hsiu-Hsien Lin, Juan Mena-Parra, B. W. Meyers, D. Michilli, Moritz Münchmeyer, Cherry Ng, Emily Petroff, Ziggy Pleunis, Mubdi Rahman, Pranav Sanghavi, Paul Scholz, Kaitlyn Shin, Ingrid H. Stairs, Shriharsh P. Tendulkar, Keith Vanderlinde, and Andrew Zwaniga. CHIME/FRB Catalog 1 Results: Statistical Cross-correlations with Large-scale Structure. *ApJ*, 922(1):42, November 2021. [arXiv:2106.04354](#), [\[DOI\]](#), [\[ADS\]](#).